

# Out-of-plane scattering at sidewall roughness in photonic crystal slabs

Wim Bogaerts, Peter Bienstman and Roel Baets

Ghent University – IMEC, Department of Information Technology (INTEC)  
Sint-Pietersnieuwstraat 41, 9000 Gent, BELGIUM

*We have simulated the effect of sidewall roughness in photonic crystal slabs using a 2-D approximation. The scattering off a sidewall irregularity is modelled as a radiating dipole excited by the incident slab mode. We studied the effect of the vertical index contrast in the slab layer to establish the impact of irregularities in high and low vertical index contrast structures respectively. It turns out that losses due to roughness are significantly larger for structures with a low refractive index contrast (like GaAs/AlGaAs or InGaAsP/InP waveguides) compared to structures with a high vertical index contrast (like Silicon-on-insulator or membranes).*

## Introduction

A promising application of photonic crystals is their use in planar waveguide structures. In photonic crystal slabs, light is controlled in-plane by a 2-D photonic crystal, like a lattice of etched holes, while in the vertical direction, light is guided through total internal reflection by either a high or a low refractive index contrast [1,2]. Due to the photonic crystal structure, the vertical confinement is not perfect, and light can leak away into the cladding. These out-of-plane losses are closely related to the choice of the layer structure. Even perfect photonic crystal slabs can have intrinsic losses when the Bloch modes are not fully confined [3]. In real structures, fabricated with lithography and dry etching, these intrinsic losses are augmented with scattering at sidewall irregularities. Again, the vertical layer structure plays a role.

## Out-of-plane scattering losses

It has been shown that intrinsic scattering losses increase dramatically with higher refractive index contrast between the slab core and cladding [4]. Therefore, one can choose a low refractive index contrast, like the GaAs/AlGaAs system. Although this structure is not lossless, losses can be kept within reason. Alternatively, layer structures with a high refractive index contrast, like silicon-on-insulator or membranes, can support lossless modes in a photonic crystal waveguide [5]. However, a breach in periodicity might cause large scattering losses. It therefore depends on the application which structure is optimal to reduce intrinsic losses [6].

Intrinsic losses only give a lower limit of the overall losses. In structures with etched holes, sidewall roughness will cause additional scattering. We studied the general effect of the vertical index contrast on these scattering losses by modelling sidewall irregularities as radiating dipoles excited by the guided light. In our 2-D approximation, air slots in a slab waveguide replace a photonic crystal slab (Figure 1). The simulations were done for the TE polarisation ( $E$ -field parallel with layer interfaces) at a wavelength of 1550nm. The total power lost due to roughness at the sidewall will be proportional to the power loss of an irregularity averaged over any position  $y$  along the interface:

$$L_{tot} \sim \int_y P(y).L(y).dy, \quad (1)$$

with  $P(y)$  the scattered power of the dipole at position  $y$ , and  $L(y)$  the fraction of that power that is not recaptured by the waveguide. Because the dipole is excited by the incident field,  $P(y)$  can be written as a function of the local field  $E(y)$ :

$$P(y) = \eta(y)^2 \cdot \frac{E^2(y)}{2Z_{rad}(y)}, \quad (2)$$

with  $\eta(y)$  describing the effect of the roughness geometry on the interface, and  $Z_{rad}(y)$  the radiative impedance of the environment.  $E(y)$  is given by the guided slab mode.

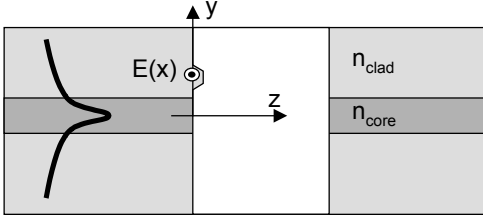


Figure 1: Out-of-plane scattering in a single air slot. The roughness is treated as a radiating dipole.

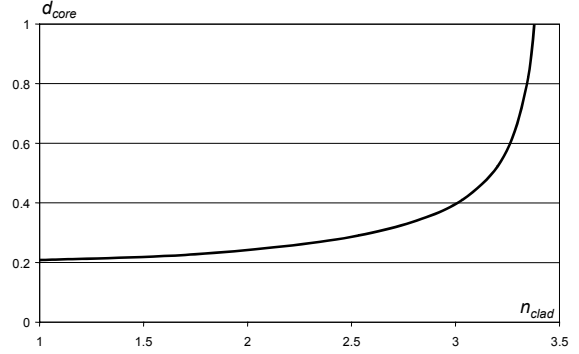


Figure 2: Waveguide core width  $d_{core}$  as a function of cladding index  $n_{clad}$  for a constant  $v$ -number.

## Simulations

We use 3 simulations to calculate the different factors in this model. First, we determine  $E(y)$  and  $Z_{rad}(y)$  by simulating the response of a dipole current source on the interface. Then we approximate  $\eta^2$  by simulating the dipole from an irregularity on an interface excited by a plane wave. Finally, we calculate the local  $E$ -field from the slab mode.

For the different simulations we used CAMFR [7,8], a vectorial eigenmode expansion tool with perfectly matched layer (PML) boundary conditions. Along the propagation axis, the structure is divided into sections with a constant refractive index profile, in which the electromagnetic field is expanded into the local eigenmodes. Radiation modes are supported through PML absorbing boundary conditions. At the interface between sections, mode matching is used to decompose the field into the eigenmodes of the new section. This way, a scattering matrix describing the entire structure is obtained.

To compare slabs with different vertical index contrast, we used three-layer symmetric slab waveguide with a  $v$ -number of 2.79 to guarantee the single-mode behaviour. The  $v$ -number is related to the refractive index contrast and the thickness of the waveguide:

$$v = k_0 \cdot d_{core} \cdot \sqrt{n_{core}^2 - n_{clad}^2}. \quad (3)$$

To keep the  $v$ -number constant, the core thickness  $d_{core}$  increases with the cladding index  $n_{clad}$ , as illustrated in Figure 2. For compatibility with both GaAs/AlGaAs and Silicon-based structures, the index of the core  $n_{core} = 3.45$  was chosen.

In the TE polarisation, a 2-D dipole radiates in all directions. Therefore, the slab core will recapture a fraction of the power. In a photonic crystal the forward and backward propagating light is coupled, so the recaptured light in both forward and backward direction is considered not lost. The fraction of lost light  $L(y)$  can be expressed as

$$L(y) = \frac{P_0(y) - R(y) - T(y)}{P_0(y)}, \quad (4)$$

with  $R(y)$  and  $T(y)$  the power in the forward and backward propagating guided mode, and  $P_0(y)$  the dipole power. We calculate this by putting a dipole current source with a known current  $I_0$  on the interface at position  $y$ . The power  $P_0(y)$  emitted by this source is

$$P_0(y) = \frac{I_0 \cdot E_0(y)}{2} \quad (5)$$

where  $E_0(y)$  is the electric field at the position of the source. As this is a 2-D simulation,  $P_0$  is measured in [W/m]. Likewise, the radiative impedance of the environment

$$Z_{rad}(y) = \frac{E_0(y)}{I_0}, \quad (6)$$

is expressed in [ $\Omega/m$ ]. Figure 3 shows  $L(y)$  for different values of  $n_{clad}$ . If the dipole is located near the slab core, a larger fraction of light is recovered. Also, a slab waveguide with high vertical index contrast can recapture more light.

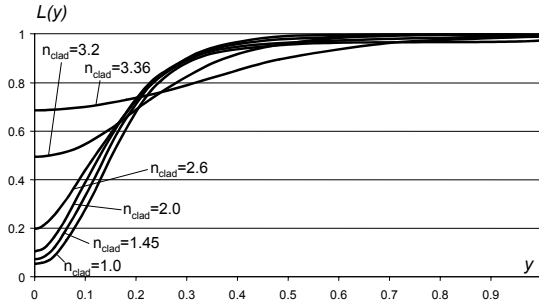


Figure 3: Loss of a radiation dipole as a function of position  $y$ .  $L(y)$  is the fraction that cannot be recaptured by the waveguide.

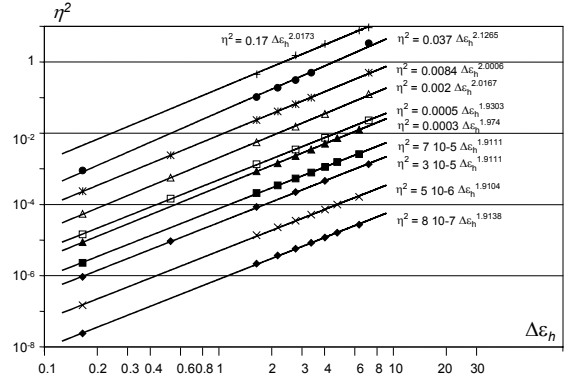


Figure 4: Strength of a dipole excited by a plane wave incident on an irregularity on a material-air interface, plotted as a function of the horizontal index contrast  $\Delta\epsilon_h$  for different irregularities.

We then calculate the excitation of the dipole  $\eta^2$  by the incident field. It is obvious that the amount of scattering depends strongly on the type of irregularities and the horizontal index contrast  $\Delta\epsilon_h = n_{mat}^2 - 1$  of the sidewall, with  $n_{mat}$  the index of the material at position  $y$ . We calculate  $\eta^2$  by scattering a plane wave off an irregularity on a material-air interface. We do this for different shapes of irregularities and  $\Delta\epsilon_h$ . Figure 4 shows  $\eta^2$  as a function of  $\Delta\epsilon_h$  for different irregularities. We find that  $\eta^2$  behaves very closely like

$$\eta^2 = \gamma \cdot (\Delta\epsilon_h)^2, \quad (7)$$

with  $\gamma$  describing the influence of the shape and size of the irregularities. This relationship with  $\Delta\epsilon_h$  is also confirmed in literature for orthogonal incidence on an interface [9].

## Results and Conclusion

With  $\eta^2$  and  $Z_{rad}(y)$  we now calculate the excitation  $P(y)$  of the dipole at position  $y$ :

$$P(y) = \gamma \cdot (\Delta\epsilon_h(y))^2 \cdot \frac{E^2(y)}{2 \cdot Z_{rad}(y)}. \quad (8)$$

Note that  $\Delta\epsilon_h$  is dependent on the position  $y$ , as the index contrast of the material-air interface is higher in the slab core than in the slab cladding. Therefore, as the core index  $n_{core}$  is fixed, a low vertical index contrast implies a high value of  $\Delta\epsilon_h$  for the cladding.

Figure 5 shows  $P(y)$  for a different  $n_{clad}$ , with  $E(y)$  based on the guided slab mode. Overall, the dipole excitation is much stronger for low vertical index contrasts because the mode profile is much broader, and  $\Delta\epsilon_h$  in the cladding is much larger.

We now combine the results to estimate the average losses due to roughness by filling in all factors in equation (1). Figure 6 shows  $L_{tot}$  as a function of  $n_{clad}$ . There is a strong increase of losses for high values of  $n_{clad}$ , i.e. low vertical index contrast. We therefore conclude that high vertical index contrast (like SOI or semiconductor membranes) performs better with respect to losses at irregularities than low out-of-plane contrast (like GaAs/AlGaAs waveguides).

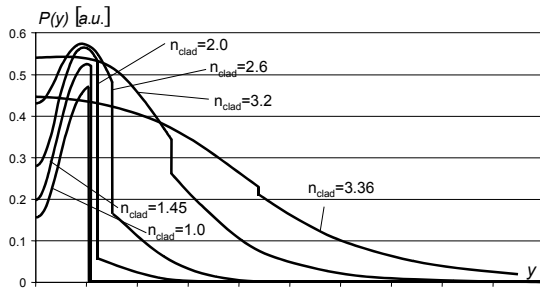


Figure 5: Power of a dipole at position  $y$  excited by the slab waveguide mode incident on a single air slot. The discontinuities occur at the core-cladding interface.

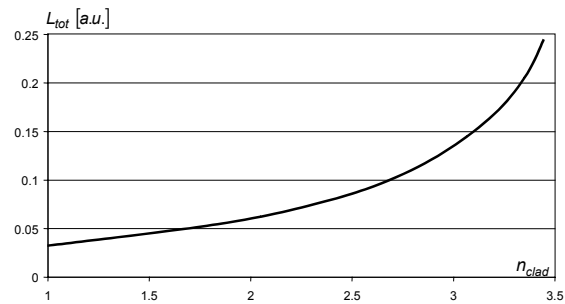


Figure 6: Average power lost due to scattering at irregularities on the sidewall of a single air slot as a function of the slab cladding index  $n_{clad}$ .

## Acknowledgements

Part of this work was carried out in the context of the European IST-PICCO project. Part of this work was carried out in the context of the Belgian IAP PHOTON network. Wim Bogaerts thanks the Flemish Institute for the Industrial Advancement of Scientific and Technological Research (IWT) for a specialisation grant. Peter Bienstman acknowledges the Flemish Fund for Scientific Research (FWO-Vlaanderen) for a postdoctoral fellowship.

## References

- [1] T.F. Krauss, R.M. DeLaRue and S. Brand, "Two-dimensional photonic-bandgap structures operating at near infrared wavelengths", *Nature* 383, p. 699, 1999
- [2] H. Bénisty, C. Weisbuch *et al.*, "Optical and confinement properties of two-dimensional photonic crystals", *J. Lightw. Technol.* 17, p. 2063, 1999
- [3] W. Bogaerts, P. Bienstman, D. Taillaert, R. Baets, D. De Zutter, "Out-of-plane Scattering in Photonic Crystal Slabs", *IEEE Phot. Technol. Lett.* (13), p.565, 2001
- [4] H. Bénisty, D. Labilloy *et al.*, "Radiation losses of waveguide-based two-dimensional photonic crystals: Positive role of the substrate", *Appl. Phys. Lett.* (76), p. 532, 2000
- [5] E. Chow, S.Y. Lin *et al.*, "Three-dimensional control of light in a two-dimensional photonic crystal slab", *Nature* 407, p. 983, 2000
- [6] W. Bogaerts, P. Bienstman, D. Taillaert, R. Baets and D. De Zutter, "Out-of-plane Scattering in 1-D Photonic Crystal Slabs", *Opt. Quant. Electron.* 34(1-3), p. 195, 2002
- [7] P. Bienstman, R. Baets, "Optical modelling of photonic crystals and VCSELs using eigenmode expansion and perfectly matched layers", *Opt. Quant. Electron.* 33(4-5), p. 327, 2001
- [8] CAMFR website: <http://camfr.sourceforge.net>
- [9] T. Germer, "Angular dependence and polarization of out-of-plane optical scattering from particulate contamination, subsurface defects, and surface microroughness", *Applied Optics* 36(33), p. 8798, 1997